

Numerical Heating in Hybrid Plasma Simulations

P. W. Rambo

University of California, Lawrence Livermore National Laboratory, P.O. Box 808, Livermore, California 94550
E-mail: pwrambo@llnl.gov

Received October 4, 1996; revised February 17, 1997

The numerical heating in hybrid particle–fluid simulations has been investigated with emphasis on the regime $ZT_e/T_i \gg 1$, where Z is the charge state of the ions and T_e and T_i are the electron and ion temperatures, respectively. For the simple case of particle ions advanced in the ambipolar field due to quasineutral isothermal fluid electrons, the heating rate is observed to be weakly dependent on time step, inversely proportional to the number of simulation particles per grid cell and strongly increasing with increasing ZT_e/T_i . Additional smoothing, due to finite Debye length, or introduced through numerical means such as higher order particle interpolation or smoothing of grid quantities, is observed to significantly reduce this heating. Both one- and two-dimensional results are presented. These results are important to hybrid particle simulations of laser generated plasmas, a regime where $ZT_e/T_i \gg 1$ is often encountered. As a relevant example, simulations of stimulated Brillouin scattering are presented illustrating the deleterious effect of numerical heating and attendant distortions to the particle distribution function. © 1997 Academic Press

I. INTRODUCTION

Hybrid simulations, which model some physical species with particles and others with fluids, have been applied to a wide variety of problems in magnetically confined fusion plasmas and space plasma physics. Typically the regime of interest is such that the ions are essentially collisionless and require a kinetic treatment while the electrons may be represented by a fluid. These models often make use of a reduced treatment of the electrons to enable efficient simulation of longer time scales. In particular, to escape restrictions due to the electron plasma frequency, quasineutrality or equilibrium Boltzmann electrons [1] are often assumed. Further approximations, such as the Darwin approximation to electromagnetics, may be used to remove restrictions due to the Courant limit on light waves; the literature reports a wide variety of specific implementations [2] with emphasis on time stability which is an important concern for these algorithms. More recent work [3] has reported on effects of the finite spatial grid; analysis and simulation elucidated an instability present for $ZT_e/T_i \gg 1$, where Z is the ion charge state and T_e and T_i are the electron and ion temperatures, respectively. The parameter ZT_e/T_i is the square of the ratio of the ion

acoustic speed, $C_s \equiv (ZT_e/M)^{1/2}$, to the ion thermal velocity, $v_{ti} \equiv (T_i/M)^{1/2}$, M is the ion mass. Instability is caused by interaction of the physical ion acoustic wave with aliases created by the spatial grid and restricts the maximum value of ZT_e/T_i for stable simulation. This restriction is particularly relevant to recent applications to laser generated plasmas including simulations of colliding plasmas [4, 5] and stimulated Brillouin scattering [6–8]. Even when ZT_e/T_i is below the threshold for finite grid instability, however, artificial heating is observed which is deleterious to accurate simulation. This heating is the subject of this work.

We consider the simple case of isothermal electrons, with constant temperature T_e . Clearly, such systems do not conserve energy, since the electrons are effectively in thermal contact with an outside energy source. In plasma expansions, for example, energy is transferred from the (inexhaustible) electron thermal energy to ion kinetic energy through the ambipolar field. In equilibrium situations, however, the ion energy should simply fluctuate about constant energy. In contrast, simulations show the ion energy to increase nearly linearly in time; this behavior is similar to the electron heating observed in models which explicitly solve the Poisson equation [9, 10]. This heating, and attendant distortion to the velocity distribution, is an important concern for accurate simulation of wave–particle interaction physics.

Simplified periodic systems are considered, consisting of particle ions with charge Ze and mass M . In the absence of collisions and magnetic field, the position and velocity of the ions are advanced simply by

$$\frac{d\mathbf{x}}{dt} = \mathbf{v}, \quad \frac{d\mathbf{v}}{dt} = \frac{Ze\mathbf{E}}{M}.$$

The electric field, \mathbf{E} , is determined from some suitable field equation and interpolated from the grid to the particles. This field equation, in turn, depends on the density accumulated from the particles by interpolation to the grid. Numerically, these are advanced in time with finite time step Δt using a leapfrog scheme with \mathbf{x} , \mathbf{E} , and density n at integer time level and velocity \mathbf{v} at the half-time step level. In Section II we will consider the simplest case of quasineu-

tral systems, where the electric field is determined from the electron pressure gradient. The numerical heating and its dependence on time step, particle number, interpolation scheme, and ZT_e/T_i will be considered. Additionally, the effect on multiple ion species, and an alternative algorithm based on energy conservation rather than momentum conservation are discussed. In Section III, the beneficial effect of smoothing is demonstrated; smoothing can be introduced through the additional physics of finite Debye length, or by explicitly adding numerical smoothing in quasineutral systems. Section IV concludes with a summary and a relevant example from simulations of stimulated Brillouin scattering.

II. NUMERICAL HEATING IN QUASINEUTRAL SIMULATION

Consider first a simple one-dimensional periodic system, with uniform spatial grid defined by $X_j = j \Delta x$, Δx the grid spacing. The ions of charge Ze and mass M are represented by particles whose density is accumulated to the grid using standard particle in cell weighting, with shape function $S(X_j - x)$ [11]. The electric field on the grid, E_j , is interpolated back to the particles in a similar way to evaluate the acceleration. With the assumption of quasineutrality, the electric field is defined by neglecting inertia in the electron momentum equation and balancing the electric force against the pressure force. In the absence of magnetic fields and assuming no current, this electric field is given by

$$E = \frac{-T_e}{en_e} \frac{\partial n_e}{\partial x} = \frac{-T_e}{en_i} \frac{\partial n_i}{\partial x}, \quad (1)$$

where the electron and ion charge densities are approximately equal due to the assumption of quasineutrality, $n_e \approx Zn_i$. The following spatial differencing has been adopted,

$$E_{j+1/2} = \frac{-T_e}{e} \frac{(n_{j+1} - n_j)}{\Delta x(n_{j+1} + n_j)/2}, \quad (2)$$

$$E_j \equiv \frac{1}{2}(E_{j+1/2} + E_{j-1/2})$$

which is identical to that used in Refs. [4, 6]. It is easily shown that this implementation exactly conserves ion momentum.

Figure 1 shows a typical example, illustrating the nearly linear increase in ion kinetic energy with time and attendant distortion to the velocity distribution function, which is no longer a Maxwellian. For this case the system length is $100 \Delta x$, the time step is $C_s \Delta t/\Delta x = 0.2$, and $ZT_e/T_i = 16$. The particles are loaded as an initially uniform Maxwellian distribution with zero drift velocity, represented by $N_p = 400$ particles per cell; linear interpolation between particles

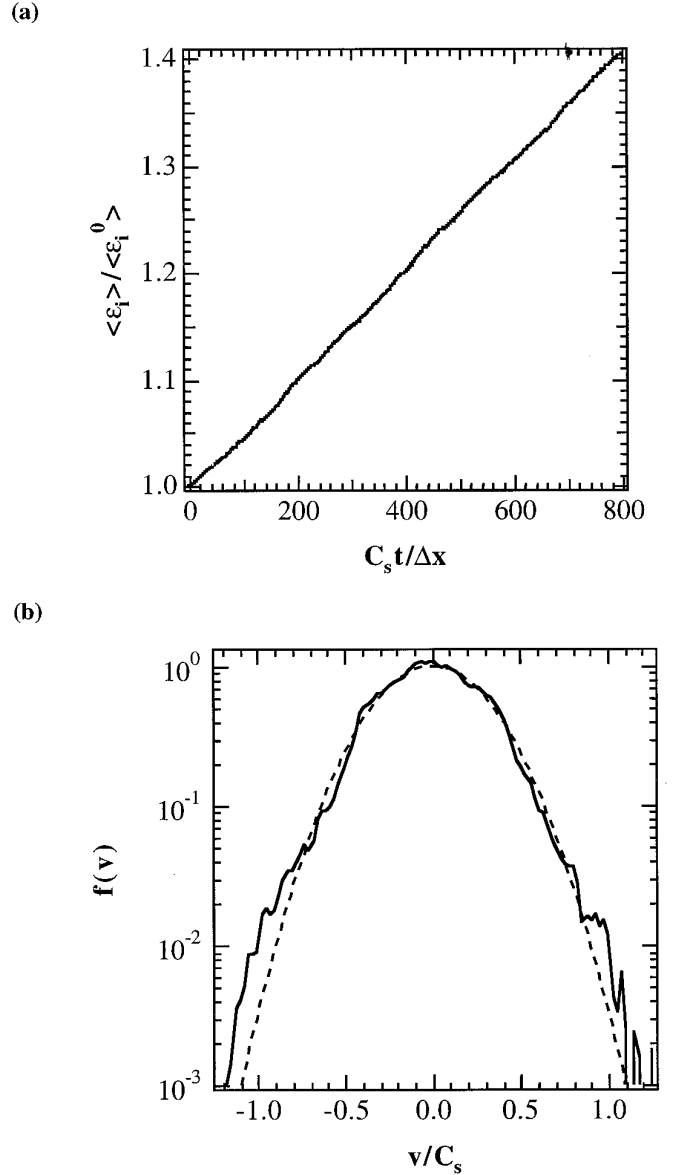


FIG. 1. Results from a one-dimensional quasineutral simulation for $ZT_e/T_i = 16$: (a) time history of kinetic energy; (b) particle distribution function at $C_s t/\Delta x = 800$ (dashed line shows Gaussian with temperature corresponding to average ion energy). Linear interpolation is used, $C_s \Delta t/\Delta x = 0.2$, and $N_p = 400/\text{cell}$.

and grid is used. This simulation has been run for a time $C_s t/\Delta x = 800$, or eight transit times for a sound wave to cross the system length. The kinetic energy plotted in Fig. 1a includes only the x -directed velocities, since in this one-dimensional example the other two components are constant. As we will see shortly, this 40% increase in the kinetic energy is inversely proportional to the number of particles per cell (keeping physical parameters constant) and is nearly independent of the time step size.

The constant rate of energy increase observed in Fig. 1

suggests that the heating is stochastic in origin [9]. Then the rate of change of the average kinetic energy of the ions, $\langle \varepsilon_i \rangle$, can be expressed as

$$\frac{d\langle \varepsilon_i \rangle}{dt} = \frac{Z^2 e^2}{M} \langle \delta E^2 \rangle \tau_c, \quad (3)$$

where $\langle \delta E^2 \rangle$ is the ensemble average of the square magnitude of the electric field fluctuations and τ_c is the relevant correlation time. For the quasineutral field solve considered here, the electric field fluctuations may be expressed in terms of the density fluctuations, $\langle \delta E^2 \rangle \approx (T_e/e \Delta x)^2 \langle (\delta n/n)^2 \rangle$. With the density fluctuations determined by the random shot noise set by the number of simulation particles per cell, $\langle (\delta n/n)^2 \rangle \approx 1/N_p$, we then obtain the normalized rate of average energy increase,

$$\eta \equiv \frac{d(\langle \varepsilon_i \rangle / \langle \varepsilon_i^0 \rangle)}{dt(C_s/\Delta x)} \propto \frac{1}{N_p} \left(\frac{ZT_e}{T_i} \right) \left(\frac{\tau_c C_s}{\Delta x} \right). \quad (4)$$

Here the normalized heating rate η is expressed in terms of the characteristic time $\Delta x/C_s$ and the initial kinetic energy, $\langle \varepsilon_i^0 \rangle$, where $\langle \varepsilon_i^0 \rangle = T_i/2$ in one dimension and $\langle \varepsilon_i^0 \rangle = T_i$ in two dimensions. If the correlation time is set by the time to cross a grid cell at the ion-acoustic wave speed ($\tau_c \approx \Delta x/C_s$), then we can anticipate that the normalized heating rate will scale linearly with ZT_e/T_i . If the correlation time τ_c is determined by the grid crossing time of particles [10], then this correlation time should scale as $\Delta x/v_{ti}$, where $v_{ti} = (T_i/M)^{1/2}$ is the ion thermal velocity; in this case we can expect $\eta \propto (ZT_e/T_i)^{3/2}$. This strong increase of the heating rate with increasing ZT_e/T_i may be countered by increasing the number of particles per cell, N_p .

The results of a series of simulations are presented in Fig. 2, showing the strong dependence on ZT_e/T_i . These simulations are all initialized with a Maxwellian distribution, uniform in space and with zero drift velocity relative to the grid. Four sets of simulations are presented: a pair using linear interpolation between particles and grid for one and two dimensions and a pair using quadratic interpolation for both one and two dimensions. The large decrease in heating obtained by using quadratic spline interpolation is obvious. Simulations with nearest grid point (NGP) interpolation were also performed indicating an approximate factor of 6 increase in heating rate, compared to linear weighting. The one-dimensional simulations were systems of length $100 \Delta x$, while the two-dimensional simulations made use of 32×32 systems with $\Delta x = \Delta y$. Each of the four sets used a constant number of particles: $N_p = 400/\text{cell}$ for linear weighting in one dimension and $N_p = 50/\text{cell}$ for the other three sets. All four sets of simulations fixed the Courant number at $\nu = C_s \Delta t/\Delta x = 0.2$. The linear dependence on the number of particles per cell was

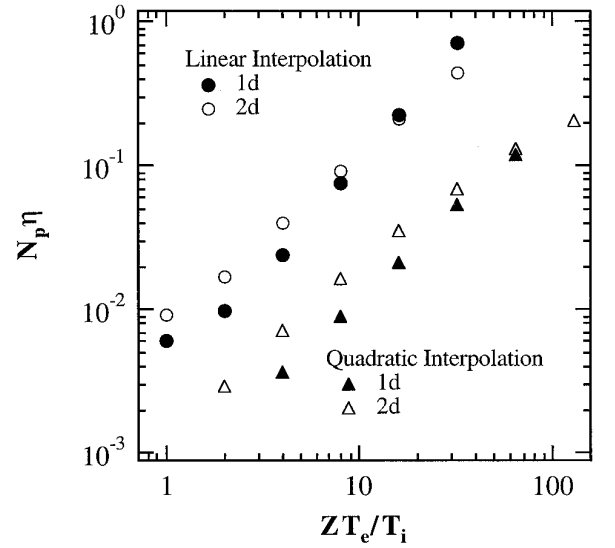


FIG. 2. Normalized heating rate as a function of ZT_e/T_i for quasineutral simulations for linear interpolation (circles) and quadratic spline interpolation (triangles); both one-dimensional (closed symbols) and two-dimensional (open symbols) simulations are shown.

confirmed by running several one-dimensional simulations with $ZT_e/T_i = 16$ and varying N_p from 50 to 400; only a 20% variation in the normalized heating rate $N_p \eta$ was observed. We should also consider the effect of finite time step, Δt . The time step is typically set by the Courant condition of resolving $\Delta x/C_s$ and, hence, for large $ZT_e/T_i > 1$ the particle motion is typically quite well resolved, i.e., $v_{ti} \Delta t/\Delta x \ll 1$, suggesting a weak dependence on time step. This weak dependence was confirmed by varying the Courant number over the range $\nu = 0.05\text{--}0.8$, resulting in roughly a 10% change in heating rate ($ZT_e/T_i = 16$, $N_p = 200$).

Some comments on these results are in order. The scaling with ZT_e/T_i is close to the three-halves power for the one-dimensional results, while the two-dimensional runs scale more nearly linearly; this range of scaling is consistent with the arguments following Eq. (4) concerning correlation time. Because the heating scales with the characteristic time $\Delta x/C_s$, increasing spatial resolution incurs a substantial computational cost for equivalent levels of numerical heating. To maintain the same fractional energy increase while halving the grid size in one dimension requires quadrupling the number of particles: a factor of 2 to maintain the same number of particles per cell and another factor of 2 because of the doubling of the physical time relative to $\Delta x/C_s$. Assuming that the Courant number is held constant so that twice as many time steps are necessary, the computational work is increased a factor of 8.

The beneficial effect of higher-order interpolation on energy conservation has also been observed in simulations

explicitly solving the Poisson equation [12]; Vu has made use of quadratic interpolation in his hybrid simulation [8]. An assessment of the benefit from higher order interpolation compared with the increased computational cost should be made in the context of the particular parameters being simulated.

As an alternative to the momentum conserving scheme presented here, a scheme similar to the “energy conserving” algorithms [13] has also been tried. In these algorithms, the force is defined by differentiating the potential energy with respect to the particle position; this involves a gradient of the particle shape function that is performed analytically and so is exact. For the case of full electron dynamics, an exact energy conservation relation is obtained in the limit of continuous time; in practice, good energy conservation requires very small time step. This prescription is equivalent to simply interpolating the electric field $E_{j+1/2}$ from the half grid positions with the interpolation reduced one order; e.g., if the density is accumulated using linear weighting, then $E_{j+1/2}$ is interpolated back to the particles using nearest grid point weighting from $X_{j+1/2}$. Numerical investigations for such an algorithm applied to the quasineutral system considered here gave results similar to those reported for explicit electron systems: ion heating can be significantly reduced, but at the price of nonconservation of momentum. The requirements on the time step are not restrictive for nondrifting plasma, most likely because for large ZT_e/T_i the particle thermal motion is well resolved for a reasonable Courant number. In fact the normalized heating rate η decreases with increasing ZT_e/T_i for a fixed Courant number. If the plasma is drifting relative to the grid ($u_0 \approx C_s$), however, the heating can be comparable to the usual momentum conserving algorithm unless the time step is reduced. A more important concern is the nonconservation of momentum, which is independent of time step. For example, simulations with $ZT_e/T_i = 16$, $N_p = 50$, and linear weighting were observed to slow down with a rate of approximately $\nu \approx 6 \times 10^{-3} C_s/\Delta x$ for $0 < u_0/C_s < 0.5$. Similar to the effect on heating in the normal momentum conserving algorithm, increasing the number of particles or the interpolation order decreases the rate of momentum loss.

The discussion so far has considered only a single ion species, but recent applications to laser produced plasmas have simulated multiple ion species with differing charge and mass. Hybrid simulations [6–8] of stimulated Brillouin scattering (SBS) are motivated by experiments using ion mixtures intended to increase ion Landau damping through the introduction of a light species. The numerical heating of this light species is an important issue, because the ion Landau damping is a sensitive function of the ratio of thermal velocity to wave speed. Consider now a plasma composed of two ion species, denoted by subscripts l and h for light and heavy, respectively; we will restrict the discussion to the case of equal ion temperatures, simply

denoted by T_i . Equation (3) is still applicable to each species separately; making the gross assumption that the correlation time is similar for both species immediately suggests that the ratio of heating rates for heavy versus light ions will be $(Z_h/Z_l)^2(M_l/M_h)$. For a typical case of CH plasma with carbon ($Z_h = 6$, $M_h = 12m_p$) and protons ($Z_l = 1$, $M_l = m_p$), this predicts the proton heating rate will be lower than that of the carbon by a factor of three. Simulations of CH plasma (equal number densities) with $T_e = 10T_i$ show the proton heating rate to be reduced approximately a factor of 2.5–3.5 compared to the carbon heating. For systems of gold and beryllium ($Z_h = 50$, $M_h = 197m_p$; $Z_l = 4$, $M_l = 9m_p$; $T_e = 2T_i$) the ratio of heating rates is observed to be approximately 5–8, compared to this simple estimate of 7.1. The ratio of heavy to light-ion heating rates, however, was observed to be much larger for Xe-H systems ($Z_h = 44$, $M_h = 131m_p$; $Z_l = 1$, $M_l = m_p$; $T_e = 2T_i$) than predicted by this argument (14:1). This plasma differs fundamentally from those just discussed in that the light particle’s thermal velocity is larger than the sound speed, likely altering the assumption made concerning correlation times.

More important than the relative heating rates is the observation that the electric field fluctuations are typically determined primarily by the high- Z , heavy species, since $\delta n_e = Z_l \delta n_l + Z_h \delta n_h \approx Z_h \delta n_h$ for $Z_h \gg Z_l$ and number concentrations not too disparate. Hence the heating is determined largely by the number of high- Z simulation particles. Again, this has been verified in simulations. This is fundamentally different from the numerical energy equilibration observed by Lawson and Gray [14], which was driven by unequal particle weights. Thus, even though the velocity distribution of light particles is often of more importance, adequate numbers of heavy particles are required to minimize numerical heating. This suggests the strategy of using higher order interpolation only for the heavy, high- Z species and not incurring the extra cost for the light species where it is ineffective; an example will be given in the concluding section. The observations made here concerning two-species plasmas also hold true in the presence of smoothing, a subject taken up in the next section.

III. SMOOTHING

To achieve acceptably low heating rates for large ZT_e/T_i , the simulator may be driven to large numbers of particles and an attendant computational burden. An obvious remedy is to introduce some form of smoothing to reduce the stochastic error fields. The use of higher order interpolation was shown to be quite effective, however, this approach is computationally expensive. In contrast, smoothing of the grid quantities is typically negligible in computational cost. This smoothing might be in the form of physical smoothing due to finite Debye length, or intro-

duced purely numerically. In this section both approaches are considered.

An alternative to the quasineutrality condition is to assume Boltzmann electrons [1, 7, 8] and solve the nonlinear Poisson equation for the electric potential Φ ,

$$-\nabla^2\Phi = 4\pi e(Zn_i - n_e) \quad (5)$$

$$\mathbf{E} = -\nabla\Phi, \quad n_e = n_0 \exp\left(\frac{e\Phi}{T_e}\right).$$

This retains the additional physics of finite electron Debye length and, hence, includes modifications to the ion acoustic dispersion relation embodied in the linear dispersion relation $(\omega/kC_s)^2 = 1/(1 + k^2\lambda_{De}^2)$, where k is the wave number and $\lambda_{De} = (4\pi n_e e^2/T_e)^{-1/2}$ is the Debye length. This Debye shielding also reduces the high wave number spectrum which is primarily responsible for numerical heating. Figure 3a shows the time history of ion kinetic energy for the case of $ZT_e/T_i = 16$ and several value of $\lambda_{De}/\Delta x$; other parameters are $N_p = 100/\text{cell}$, linear weighting, and $C_s \Delta t/\Delta x = 0.2$. These results clearly illustrate a strong reduction in heating rate for Debye length comparable to the grid spacing. (The heating rate is little affected for $\lambda_{De}/\Delta x < 0.2$.) This would seem to be one of the rare happy occurrences where the inclusion of better physics additionally contributes to better numerical behavior.

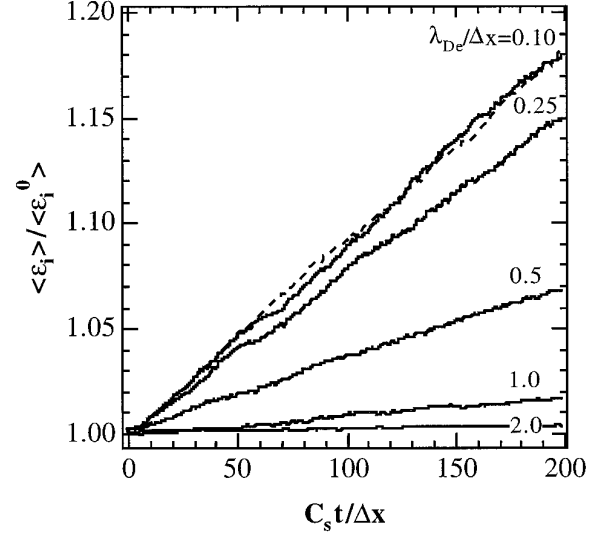
Of course, the physical system of interest may preclude setting $\Delta x \approx \lambda_D$. In fact, reducing the grid size for fixed Debye length is not generally a good strategy. For example, Fig. 3a indicates approximately a factor of 6 reduction in heating due to increasing $\lambda_{De}/\Delta x$ from 0.5 to 1.0. If this is achieved by halving the grid spacing, then the number of particles would need to be doubled to maintain constant N_p , and the number of time steps doubled to maintain a constant Courant condition; thus the computational work is quadrupled. And since the normalized time $tC_s/\Delta x$ is also doubled for equivalent physical time, the decrease in heating is only a factor of 3. For small values of the Debye length, the reduction in heating is small, and reducing the grid spacing so as to increase $\lambda_{De}/\Delta x$ will exacerbate the numerical heating.

Given this, the addition of numerical smoothing seems an attractive alternative. We consider here simple 3-point digital smoothing of the form

$$\tilde{f}_j = \frac{\alpha f_{j-1} + f_j + \alpha f_{j+1}}{1 + 2\alpha}, \quad (6)$$

where f_j is any grid quantity and α is the smoothing parameter (generally, $0 < \alpha < \frac{1}{2}$). One could directly smooth the electric field using Eq. (6) before pushing the particles, but momentum conservation is no longer guaranteed. For the quasineutral field solution expressed by Eq. (2), mo-

(a)



(b)

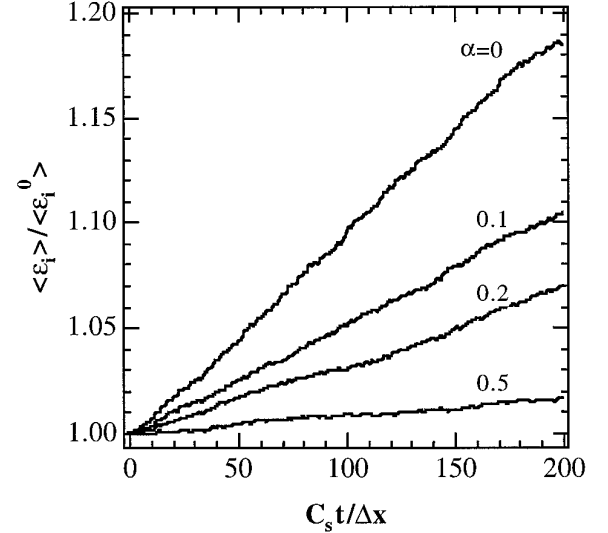


FIG. 3. Time histories of kinetic energy for simulations ($ZT_e/T_i = 16$, $N_p = 200/\text{cell}$, $C_s \Delta t/\Delta x = 0.2$) with (a) Boltzmann electrons and various values of the Debye length relative to the grid spacing, $\lambda_{De}/\Delta x$ (quasineutral stimulation, $\lambda_{De} = 0$, is shown in dotted line for comparison); (b) quasineutral simulations with smoothing of the electric field through Eq. (7) for various values of the smoothing parameter α .

mentum conservation can be retained if the density in the numerator is smoothed, but *not* the density in the denominator:

$$E_{j+1/2} = \frac{-T_e}{e} \frac{(\tilde{n}_{j+1} - \tilde{n}_j)}{\Delta x(n_{j+1} + n_j)/2}, \quad E_j \equiv \frac{1}{2}(E_{j+1/2} + E_{j-1/2}). \quad (7)$$

The linear dispersion is, of course, altered at large wave

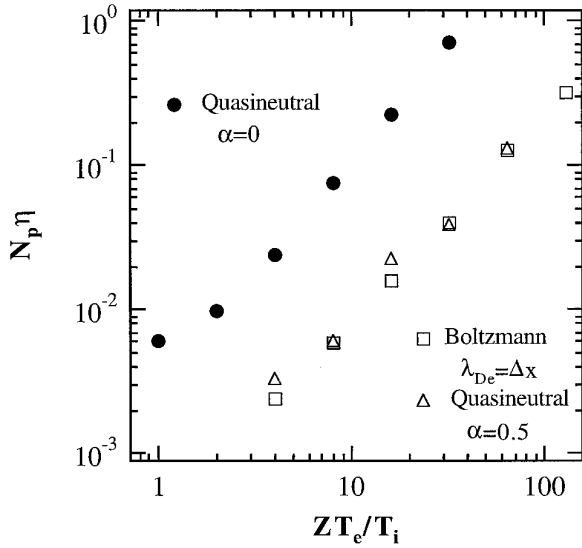


FIG. 4. Normalized heating rate as a function of ZT_e/T_i for one-dimensional simulations: quasineutral electrons without smoothing, $\alpha = 0$ (closed circles), quasineutral with smoothing, $\alpha = 0.5$ (triangles), and Boltzmann electrons, $\lambda_{De} = \Delta x$ (squares).

number. Figure 3b shows the effect of this smoothing for several values of α (otherwise, identical parameters to Fig. 3a). An alternative, more general, method that maintains momentum conservation is to symmetrically smooth both density and field [15].

The scaling results discussed in the previous section still hold true for both numerically introduced smoothing and finite Debye length. Scaling of the normalized heating rate with ZT_e/T_i is similar, as illustrated by Fig. 4 which shows results from three sets of one-dimensional simulations, all with linear weighting and $C_s \Delta t / \Delta x = 0.2$. Two sets of simulations are quasineutral, one with no smoothing ($\alpha = 0$, $N_p = 400/\text{cell}$) and one with $\alpha = 0.5$ ($N_p = 100/\text{cell}$); the third simulation set has finite Debye length, with $\lambda_{De} = \Delta x$ ($N_p = 200/\text{cell}$).

IV. CONCLUSION

To illustrate some of the deleterious effects that can arise, an example relevant to recent simulations [6–8] of stimulated Brillouin scattering is presented. The plasma of interest is a mixture of carbon and hydrogen ($Z_h = 6$, $M_h = 12m_p$; $Z_l = 1$, $M_l = m_p$) with equal number concentrations; the electron density is $n_e = 2.25 \times 10^{21} \text{ cm}^{-3}$ (quarter critical for blue laser light), with $T_e = 10T_i$ and $T_l = T_h = T_i$. The sound speed is approximately $C_s = 4.1 \times 10^7 \text{ cm/s}$, while the wave number of interest is approximately twice the incident laser wave number, $k = 2k_0 = 3.6 \times 10^5 \text{ cm}^{-1}$. Figure 5 shows the time-dependent reflectivity due to SBS for a laser intensity of $I = 5.4 \times$

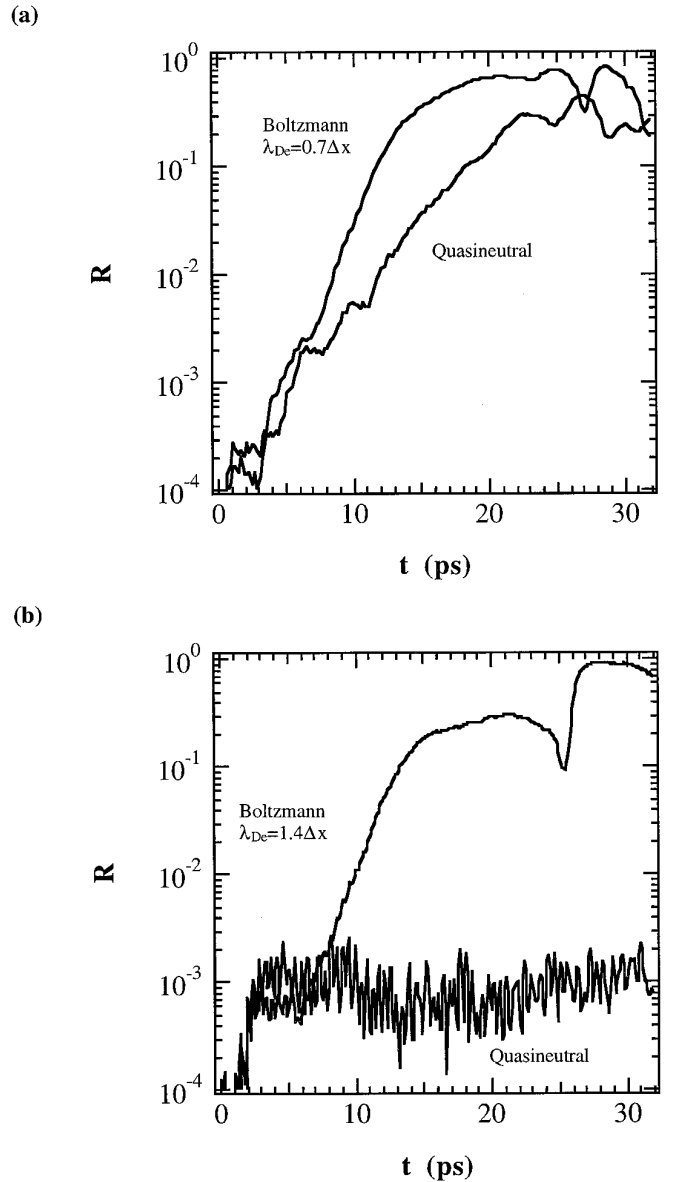


FIG. 5. Time dependent reflectivity due to stimulated Brillouin scattering from a CH plasma comparing hybrid simulations with Boltzmann electrons and quasineutral electrons for two levels of spatial resolution: (a) $k_0 \Delta x = 0.22$ ($\Delta x = 1.2 \times 10^{-6} \text{ cm}$); (b) $k_0 \Delta x = 0.11$ ($\Delta x = 6.0 \times 10^{-7} \text{ cm}$); all four simulations use linear interpolation and the same total number of simulation particles. Blue laser light with intensity $I_0 = 5.4 \times 10^{15} \text{ W/cm}^2$ is incident on a CH plasma with density $n_e = 2.25 \times 10^{21} \text{ cm}^{-3}$, temperature $T_e = 10T_i = 3.0 \text{ keV}$, and length $L = 11 \mu\text{m}$.

10^{15} W/cm^2 incident on a plasma of length $L = 11 \mu\text{m}$. These SBS simulations include an electromagnetic field solver, subcycled relative to the ion particle advance; the electron ponderomotive potential is accumulated during the electromagnetic advance and added to the electrostatic field for advancing the ions [6]. (The direct effect of the electromagnetic field on the ions is negligible because of

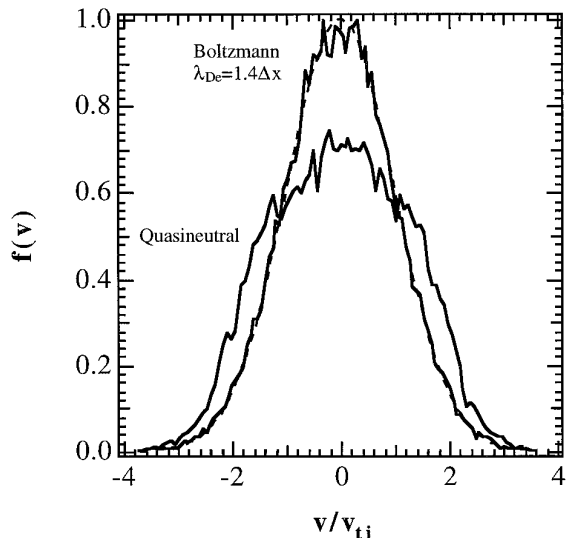


FIG. 6. Proton velocity distribution function at $t = 8.0 \text{ ps} = 540 \Delta x / C_s$ from uniform periodic simulations with Boltzmann electrons, $\lambda_{De} = 1.4 \Delta x$, and quasineutral electrons ($\lambda_{De} = 0$); dashed line shows Gaussian at initial temperature. All plasma and numerical parameters are the same as in Fig. 5b.

the disparity between electron and ion mass.) A comparison between a quasineutral run and a run with finite Debye length ($\lambda_{De}/\Delta x = 0.7$) is shown in Fig. 5a from simulations with fairly coarse resolution, $k_0 \Delta x = 0.22$ ($\Delta x = 1.2 \times 10^{-6} \text{ cm}$). These simulations were performed with linear weighting and $N_p = 400/\text{cell}$ for both carbon ions and protons (approximately 700 thousand particles total). The reflectivities are similar, with the quasineutral run growing slightly more slowly in time and peaking at a slightly lower value. The difference might be attributed to the additional physics due to finite Debye length included in the run with Boltzmann electrons; however, a different concern is raised by two runs with better spatial resolution ($k_0 \Delta x = 0.11$) and the same total number of particles, shown in Fig. 5b. The two runs with finite Debye length are similar, but the quasineutral simulations have completely diverged. The difficulty is clarified by Fig. 6, which shows the velocity distribution of protons from periodic (undriven) simulations with parameters corresponding to the better resolved case of Fig. 5b, at time $t = 8 \text{ ps} = 540 \Delta x / C_s$. The severe distortion of the distribution function due to numerical heating in the quasineutral case is evident, leading to the complete breakdown of the simulation. For the coarser resolution, the factor of two greater number of particles per cell (for constant total number) combined with the doubling of the characteristic time $\Delta x / C_s$ implies this amount of distortion to the distribution function would not have occurred until time $t = 32 \text{ ps}$. This example makes clear the beneficial effect of smoothing from finite Debye length, even though the physical difference is small, since

$k\lambda_{De} \approx 0.3 \ll 1$ for the driven ion wave. The situation can be further improved by using quadratic spline interpolation for the carbon (the heating of the protons is determined primarily by the carbon), which produces consistent results for quasineutral simulation with the finer spatial resolution. With the smoothing from finite Debye length and quadratic spline interpolation for the carbon, the number of carbon simulation particles may even be reduced; e.g., $N_p = 50/\text{cell}$ was still found to give acceptable results for the better resolved case. The increased computational cost of quadratic splines is more than offset by the fewer particles, while the more relevant proton distribution is well represented without incurring the computational cost of (ineffective) higher-order interpolation.

In summary, simulations and heuristic theory of the non-physical heating observed in hybrid particle–ion fluid–electron simulations have been presented. The scaling of the heating rate with number of particles per grid cell, time step, and with the parameter ZT_e/T_i was investigated. The strong dependence with this latter parameter is of particular importance to simulations of laser-produced plasmas, where $ZT_e/T_i \gg 1$ is often encountered. The beneficial effects of smoothing were illustrated in the three cases of smoothing due to finite Debye length, numerical grid smoothing, and higher-order particle–grid interpolation. The example of stimulated Brillouin scattering just presented clearly illustrates the difficulty in performing accurate simulations for the regime $ZT_e/T_i \gg 1$ even in one dimension; this work should help to assess the requirements for meaningful simulation in two and three dimensions.

ACKNOWLEDGMENTS

The author acknowledges helpful discussions with B. Cohen, A. B. Langdon, B. Lasinski, W. S. Lawson, and S. C. Wilks. This work was performed under the auspices of the U.S. Department of Energy by Lawrence Livermore National Laboratory under Contract W-7405-Eng-48.

REFERENCES

1. H. Okuda *et al.*, Quasi-neutral particle simulation model with application to ion wave propagation, *Phys. Fluids* **21**, 476 (1978).
2. D. W. Hewett, Low-frequency electromagnetic (Darwin) applications in plasma simulation, *Comput. Phys. Commun.* **84**, 243 (1994), and references found therein.
3. P. W. Rambo, Finite-grid instability in quasineutral hybrid simulations, *J. Comput. Phys.* **118**, 152 (1995).
4. P. W. Rambo and R. J. Procassini, A comparison of kinetic and multifluid simulations of laser-produced colliding plasmas, *Phys. Plasmas* **2**, 3130 (1995).
5. M. E. Jones *et al.*, Modeling ion interpenetration, stagnation, and thermalization in colliding plasmas, *Phys. Plasmas* **3**, 1096 (1996).
6. Wilks *et al.*, Nonlinear theory and simulations of stimulated Brillouin backscatter in multispecies plasmas, *Phys. Rev. Lett.* **74**, 5048 (1995).

7. B. I. Cohen, B. F. Lasinski, A. B. Langdon, and E. A. Williams, Resonantly excited nonlinear ion waves, *Phys. Plasmas*, to appear.
8. H. X. Vu, An adiabatic fluid electron particle-in-cell code for simulating ion-driven parametric instabilities, *J. Comput. Phys.* **124**, 417 (1996).
9. R. W. Hockney, Measurements of collision and heating times in a two-dimensional thermal computer plasma, *J. Comput. Phys.* **8**, 19 (1971).
10. H. Abe, J. Miyamoto, and R. Itatani, Grid effects on the plasma simulation by the finite-sized particle, *J. Comput. Phys.* **19**, 134 (1975).
11. C. K. Birdsall and A. B. Langdon, *Plasma Physics via Computer Simulation* (McGraw Hill, New York, 1985).
12. H. Abe, N. Sakairi, R. Itatani, and H. Okuda, High-order spline interpolations in the particle simulation, *J. Comput. Phys.* **63**, 247 (1986).
13. A. B. Langdon, "Energy-conserving" plasma simulation algorithms, *J. Comput. Phys.* **12**, 247 (1973); C. Birdsall and A. B. Langdon, *op. cit.*, pp. 213–233 and references found therein.
14. W. S. Lawson and P. C. Gray, Heat flow between species in one-dimensional particle plasma simulations, *J. Comput. Phys.* **95**, 195 (1991).
15. A. B. Langdon, private communication, February 24, 1994.